Molecular Neurobiology (2019) 56:4203–4214
https://doi.org/10.1007/s12035-018-1366-4

Effects of Neutralizing Antibody Production on AAV-PHP.B-Mediated Transduction of the Mouse Central Nervous System

Yoichiro Shinohara[1,2] · Ayumu Konno[1] · Keisuke Nitta[1,2] · Yasunori Matsuzaki[1] · Hiroyuki Yasui[1] · Junya Suwa[3] · Keiju Hiromura[3] · Hirokazu Hirai[1,4]

Received: 23 February 2018 / Accepted: 25 September 2018 / Published online: 5 October 2018

Abstract

Adeno-associated virus (AAV)-PHP.B, a capsid variant of AAV serotype 9, is highly permeable to the blood-brain barrier. A major obstacle to the systemic use of AAV-PHP.B is the generation of neutralizing antibodies (NAbs); however, temporal profiles of NAb production after exposure to AAV-PHP.B, and the influence on later AAV-PHP.B administration, remains unknown. To address these, AAV-PHP.Bs expressing either GFP or mCherry by neuron-specific or astrocyte-specific promoters were intravenously administered to mice at various intervals, and brain expression was examined. Injection of two AAV-PHP.Bs, separated temporally, showed that as little as a 1-day interval between injections resulted in a significant decrease in expression of the second transgene, with a complete loss of expression after 7 days, paralleling an increase in serum NAb titers. Brain parenchymal injection was explored to circumvent the presence of NAbs. Mice systemically pre-treated with an AAV-PHP.B were injected intra-cerebrally with an AAV-PHP.B expressing GFP. After 2 weeks, marked GFP expression in the cerebellum was evident, showing that pre-existing NAbs did not affect the AAV-PHP.B directly injected into the brain. In contrast, reversing the injection order, i.e., cerebellar injection followed by systemic injection, completely eliminated expression of the second transgene. We confirmed that intra-cerebellar injection produced NAbs in the serum, but not in the cerebrospinal fluid (CSF). Our results indicate that the preclusion of brain transduction by a second AAV-PHP.B administration begins from the first day following systemic injection and is established within 1 week. Serum NAbs can be avoided by directly injecting AAV-PHP.Bs into brain tissue.

Keywords Adeno-associated virus · AAV-PHP.B · Cell type-specific promoter · ELISA · Neutralizing antibody

Introduction

Adeno-associated virus (AAV) is a member of the *Parvoviridae* family that was originally identified in simian adenovirus preparations [1]. It is one of the smallest known viruses (20–25 nm in diameter) having a non-enveloped capsid [2]. In humans, infection with AAV causes no symptoms or diseases. The AAV genome consists of a linear single-stranded DNA approximately 4.7 kb in length, containing two long inverted terminal repeats (ITR) at the termini [2]. In various species, including humans, vectors derived from most serotypes of AAV are able to efficiently transduce both neurons and glial cells in a wide range of central nervous system (CNS) regions [3, 4]. Administration of AAV vectors directly into brain tissue, through either the sub-arachnoidal space or the cerebral ventricle, causes a broad transduction of the brain [5–7], whereas intravenous injection results in little or no brain transduction, largely because of the limited penetration of AAV through the blood-brain barrier (BBB) [8–10].

Yoichiro Shinohara and Ayumu Konno contributed equally to this work.

Electronic supplementary material The online version of this article (https://doi.org/10.1007/s12035-018-1366-4) contains supplementary material, which is available to authorized users.

✉ Hirokazu Hirai
hirai@gunma-u.ac.jp

[1] Department of Neurophysiology and Neural Repair, Gunma University Graduate School of Medicine, Maebashi, Gunma 371-8511, Japan

[2] Department of Ophthalmology, Gunma University Graduate School of Medicine, Maebashi, Gunma 371-8511, Japan

[3] Department of Nephrology and Rheumatology, Gunma University Graduate School of Medicine, Maebashi, Gunma 371-8511, Japan

[4] Research Program for Neural Signaling, Division of Endocrinology, Metabolism and Signal Research, Gunma University Initiative for Advanced Research, Maebashi, Gunma 371-8511, Japan

Recently, Deverman et al. reported that, in mice, AAV-PHP.B, a capsid variant of AAV9 carrying a seven-amino acid insertion, showed greater permeability of the BBB compared to AAV serotype 9 (AAV9) [11]. Previously, we have succeeded in obtaining a highly efficient, specific, transduction of cerebellar Purkinje cells upon intravenous injection of AAV-PHP.B carrying a Purkinje cell-specific L7-6 promoter [12], suggesting the promise of using AAV-PHP.B, in combination with a cell type-specific promoter, for venous-mediated transgene delivery and expression in specific cell populations within the CNS. In combination with miRNA expression or genome-editing techniques, AAV-PHP.B could therefore allow highly efficient knock-down or knock-out of target genes, or knock-in of a gene of interest, into a target genomic site simply by intravenous injection. Such an approach would be highly valuable in basic neuroscience research, as well as offering the potential for future clinical application using gene therapy to treat various genetic diseases that affect the brain.

However, a major concern over the use of this approach is the presence of neutralizing antibodies that are produced in response to natural infection by AAV, or as a result of the therapeutic use of AAV vectors, which would prevent infection. If this were the case, the circulation-mediated delivery of AAV-PHP.B to the CNS may be available only once (or none) per animal (or human) as long as humoral immunity is maintained. Thus, presence of NAbs will exclude the use of AAV in gene therapy both pre-clinically, as well as clinically. The relationship between the time course of neutralizing antibody production upon first AAV-PHP.B administration and the subsequent inhibitory effect of CNS transduction following a second intravenous injection of AAV-PHP.B remains to be explored. In this study, we examined the potential use and limitations of AAV-PHP.B-mediated gene transfer into the CNS.

Materials and Methods

Animals

Wild-type C57BL/6 mice between 4 and 5 weeks of age were bred at the Gunma University Bioresource Center (Maebashi, Gunma, Japan) for use in this study. Mice were maintained on a 12-h light/dark cycle and had access to food and water ad libitum. All efforts were made to minimize animal suffering, and the number of animals used was reduced. All procedures for animal care and treatment were approved by Gunma University Animal Care and Experimentation Committee (No. 17-026).

Production of AAV-PHP.B Vectors

The 0.6-kb astrocyte-specific mouse ABC1D glial fibrillary acidic protein (mGFAP) promoter [13, 14] and the 1.2-kb rat neuron-specific enolase (rNSE) promoter [15] were inserted into XhoI/AgeI-digested pAAV-GFP AAV vector. The mGFAP upstream promoter region of the GFAP gene was amplified by polymerase chain reaction (PCR) from mouse genomic DNA using the following two pairs of primers: 5′-ATGCTCTAGACTCGAGACGCGTAACAAATACC ATGTCGCTGG-3′, 5′-GAACTCCCCAGGGTACTCGC TGAATAG-3′ and 5′-TACCCTGGGGAGTTCTCCCC CTAGCTGG-3′, 5′-CATGGTGGCGACCGGTGCGG CGCGCAGAGGTGATGCGTCTCCGCTCCAAC CTGCCCTGCCTCTGCTGGC-3′. The 1.2-kb rNSE promoter was constructed as previously reported [15]. The red fluorescent protein mCherry was inserted into AgeI/NotI-digested site of either the pAAV-mGFAP or pAAV-rNSE GFP AAV vectors.

The packaging plasmid for the AAV-PHP.B (pAAV-PHP.B) was constructed by replacing the wild-type fragment between the BsiWI and PmeI sites of pAAV2/9 (kindly provided by Dr. J. Wilson from University of Pennsylvania) with the mutant capsid gene fragment, containing the partial PHP.B VP1 gene (GenBank KU056473). This fragment was then subcloned into pAAV2/9. The AAV-PHP.B vector was produced by a triple-transfection of HEK293T cells with three plasmids: the expression plasmid, pHelper (Stratagene, La Jolla, CA, USA), and pAAV-PHP.B. The viral particles were purified using ammonium sulfate or polyethylene glycol 8000 precipitation and by iodixanol continuous gradient centrifugation, as previously described [12, 16]. The genomic titers of the purified AAV-PHP.B vectors were determined by quantitative real-time PCR using THUNDERBIRD™ SYBR® qPCR Mix (Toyobo) with the primers 5′-CTGT TGGGCACTGACAATTC-3′ and 5′-GAAG GGACGTAGCAGAAGGA-3′, targeting the woodchuck hepatitis post-transcriptional regulatory element (WPRE) sequence. The expression plasmid vectors were used as standards.

Intravenous Injection of AAV-PHP.B into the Mouse Orbital Venous Plexus

After deep anesthesia via an intra-peritoneal injection of ketamine (100 mg/kg body weight) and xylazine (10 mg/kg body weight), 100 μL of the AAV vector preparation was intravenously injected into the retro-orbital sinus of mice over a period of 1 min, using a 1-mL syringe attached to a 29-gauge needle (SS-10M2913A, TERUMO, Tokyo, Japan). The syringe was kept in place for 30 s following the injection. The same volume of PBS was injected intravenously as a control. Cerebellar and cerebral parenchymal injections were administered as previously described [6, 15]. For intracerebroventricular injections, the skin over the cerebral hemisphere was cut, and a burr hole was made 0.3 mm posterior and − 1.0 mm medial-lateral from the bregma, and the needle was inserted +

2.5 mm ventrally. Sample size and AAV genomic titer for each experiment are shown in the corresponding figures and/or results section.

Immunohistochemistry

Deeply sedated mice were transcardially perfused with phosphate-buffered saline (PBS) (pH 7.4) and 4% paraformaldehyde in 0.1 M phosphate buffer (PB). Following this, whole brains were immersed in 4% paraformaldehyde for 6 h at 4 °C and cut into 50-μm sagittal sections using a microtome (Leica VT1000 S; Leica Microsystems, Wetzlar, Germany). Free-floating sagittal brain sections were blocked with PBS containing 2% normal donkey serum, 0.1% Triton X-100, and 0.05% NaN_3 (blocking solution) and were then incubated overnight at 4 °C with primary antibodies. The primary antibodies used were rat monoclonal anti-GFP (1:1000; 04404-84; Nacalai, Kyoto, Japan), rabbit polyclonal anti-DsRed (1:1000; Rb-Af2020; Clontech, Mountain View, CA, USA), and mouse monoclonal anti-NeuN (1:1000; MAB377, Merck Millipore, Billerica, MA, USA). After washing three times with PBS at room temperature (24 °C), the slices were incubated in a blocking solution for 4 h at room temperature (24 °C) with the appropriate secondary antibody. The secondary antibodies used were Alexa Fluor 488 donkey anti-rat IgG (1:1000; Thermo Fisher Scientific, Waltham, MA, USA), Alexa Fluor 568 donkey anti-rabbit IgG (1:1000; Thermo Fisher Scientific), and Alexa Fluor 680 donkey anti-mouse IgG (1:1000; Thermo Fisher Scientific). After washing using the same procedure as above, immunostained sections were mounted on glass slides with ProLong Diamond antifade reagents (Thermo Fisher Scientific).

Imaging Analysis

Fluorescence images were acquired on a fluorescence microscope (VB-7010 or BZ-X700; Keyence, Osaka, Japan) or a confocal laser-scanning microscope (LSM 800; Carl Zeiss, Oberkochen, Germany). The GFP fluorescence images were captured using a confocal microscope with the same settings in each experimental group. Following this, the outline of the brain section was traced, and the fluorescence intensity in the enclosed areas was measured using ImageJ (http://rsbweb.nih.gov/ij/). The background intensity was subtracted from the fluorescence intensity.

Quantification of the Neutralizing Antibodies

Neutralizing antibodies against AAV-PHP.B capsid present in blood were evaluated using an enzyme-linked immunosorbent assay (ELISA), as reported previously with some modifications [17]. Maxisorp 96-well plates (442404, Thermo Fisher Scientific) were coated with AAV-PHP.B vector at 1×10^{10} vg/well using an ELISA coating buffer (421701, BioLegend, San Diego, CA, USA) overnight at 4 °C. The wells were washed three times with PBS containing 0.05% Tween 20 (washing buffer) and, then, blocked with PBS containing 10% fetal bovine serum (FBS) (blocking and sample buffer) for 2 h at room temperature (20 °C). After blocking non-specific binding, the serum dilutions were added to the wells and incubated for 2 h at room temperature (20 °C). The serums were diluted at 1:100 and 1:1250 for analysis of IgG and IgM, respectively. After washing three times, goat anti-mouse IgG-HRP (1:10,000; 12-349, Merck Millipore) or IgM-HRP (1:2000; 62-6820, Thermo Fisher Scientific) was added to the wells and then incubated for 2 h at room temperature (20 °C). After washing four times, the wells were incubated with 100 μL of 3,3′,5,5′-tetramethylbenzidine (TMB) substrate (421101, BioLegend) for 10 min, after which 50 μL of 2 N H_2SO_4 was added to stop the reaction. The absorbance values were measured using an ELISA plate reader (Wallac ARVO-SX 1420 Multilabel Counter, PerkinElmer, Waltham, MA, USA) at 450 nm. The background absorbance values were subtracted from the obtained values. The average absorbance value of samples collected 7 days after AAV-PHP.B injection was defined as 100%.

Statistical Analysis

Statistical analyses were performed using the R software statistical package (www.r-project.org). Significant differences were analyzed using a one-way analysis of variance (ANOVA) followed by Tukey's post hoc test. A p value < 0.05 was considered statistically significant. All data are shown as the mean ± SEM.

Results

Distinct Labeling of Neurons and Astrocytes with Different Fluorescent Proteins Using Transduction with AAV-PHP.Bs Carrying the Respective Cell Type-Specific Promoters

Intravenous injection of AAV-PHP.B expressing a fluorescent marker protein under the control of a cell type-specific promoter allows for the fluorescent labeling of a specific cell population. In this regard, we have succeeded in expressing GFP specifically in cerebellar Purkinje cells using AAV-PHP.B expressing GFP under the control of the Purkinje cell-specific L7-6 promoter [12]. We wished to simultaneously label different cell populations with distinct fluorescent marker proteins by intravenous administration of a mixture of AAV-PHP.Bs expressing distinct fluorescent marker proteins under the control of different cell type-specific promoters. Since we have previously reported neuron-specific

labeling using AAV9 vectors carrying the neuron-specific rNSE promoter [15] and astrocyte-specific labeling using AAV9 vectors carrying the astrocyte-specific mGFAP promoter [13, 14], we first validated whether these two promoters, in combination with AAV-PHP.B, could be used to express marker proteins in neurons and astrocytes specifically. In 4- to 5-week-old C57BL/6 mice, intravenous injection of an AAV-PHP.B vector expressing GFP under the control of the mGFAP promoter (1.0×10^{12} vg/100 μL) (Fig. 1a) caused broad transduction in the CNS 3 weeks post-injection. Immunostaining for GFP and NeuN, a neuronal marker, revealed expression of GFP specifically in astrocytes (i.e., there was no overlap with NeuN-positive neurons) (Fig. 1b–d). Similarly, an intravenous injection of AAV-PHP.B expressing GFP under the control of the rNSE promoter (1.0×10^{12} vg/100 μL) (Fig. 1e) efficiently labeled neurons in the brain, all of which could be co-stained for NeuN (Fig. 1f–h).

Following this, we mixed equal amounts of two AAV-PHP.Bs expressing different fluorescent proteins, namely mCherry under the control of the rNSE promoter (5.0×10^{12}

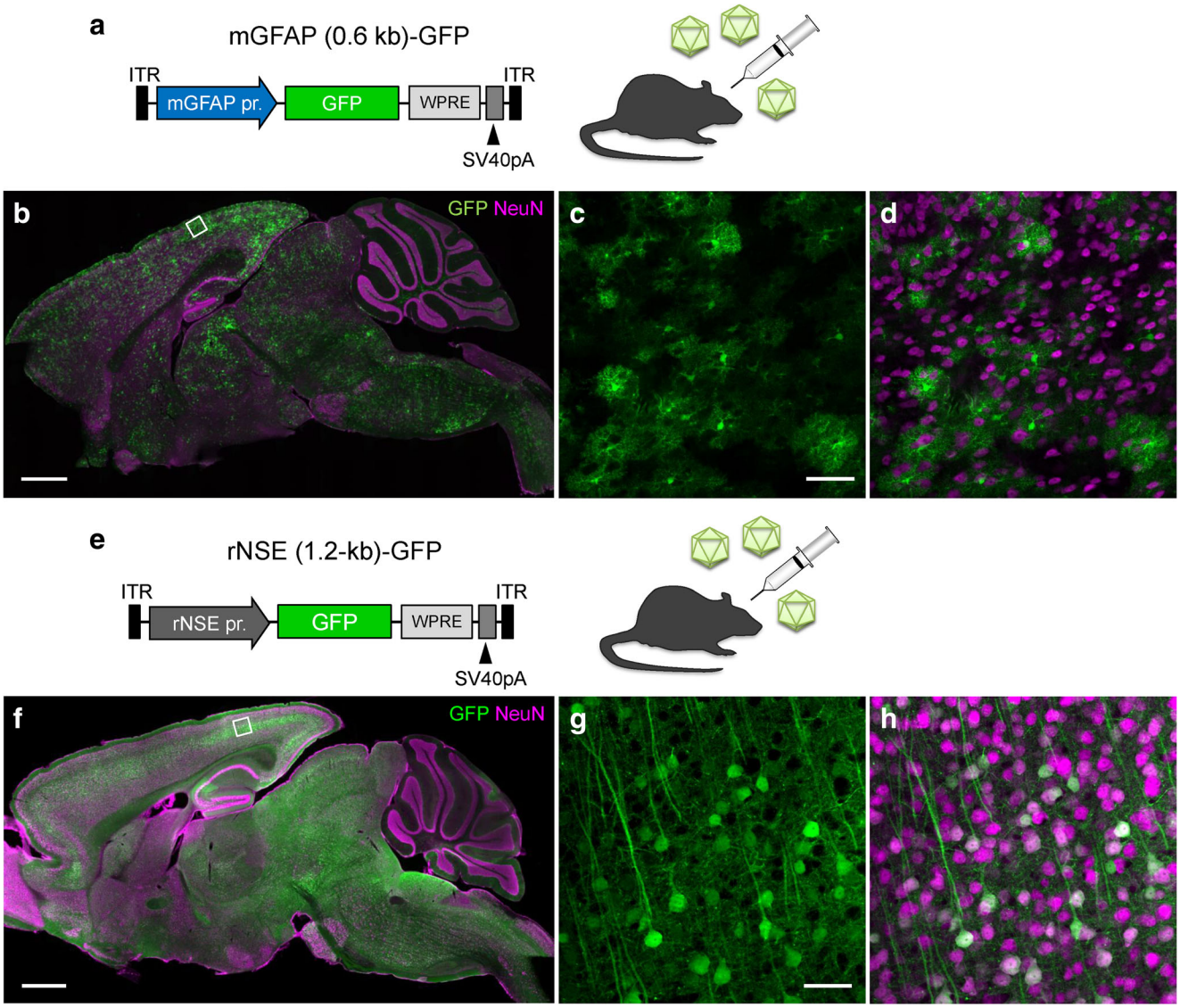

Fig. 1 Astrocyte- or neuron-specific transgene expression by AAV-PHP.B carrying the cell type-specific promoter. **a**, **e** Schema depicting the AAV vector constructs, which were designed to express GFP under the control of the 0.6-kb astrocyte-specific mGFAP promoter (**a**) or the 1.2-kb neuron-specific rNES promoter (**e**). GFP green fluorescent protein, ITR inverted terminal repeat, mGFAP mouse glial fibrillary acidic protein, rNSE rat neuron-specific enolase, SV40pA simian virus 40 polyadenylation, WPRE woodchuck hepatitis virus post-transcriptional regulatory element. AAV-PHP.B was intravenously administered to 5-week-old mice through the orbital sinus, and mice were sacrificed 3 weeks after the injection. **b**, **f** Immunohistochemistry of sagittal sections for GFP and NeuN. **c**, **d**, **g**, **h** Enlarged immunohistochemical images of the boxed regions in the cerebral cortex regions shown in (**b**) or (**f**). Fluorescent images for GFP alone (**c**, **g**) and GFP + NeuN (**d**, **h**) show the expression of GFP specifically in astrocytes (**c**, **d**) and neurons (**g**, **h**). Scale bars, 1 mm (**b**, **f**) and 50 μm (**c**, **g**)

vg in 50 μL) and GFP under the control of the mGFAP promoter (5.0×10^{12} vg in 50 μL), and the viral mixture (total 100 μL) was injected intravenously into 5-week-old mice (Fig. 2a). Three weeks after injection, the expression patterns

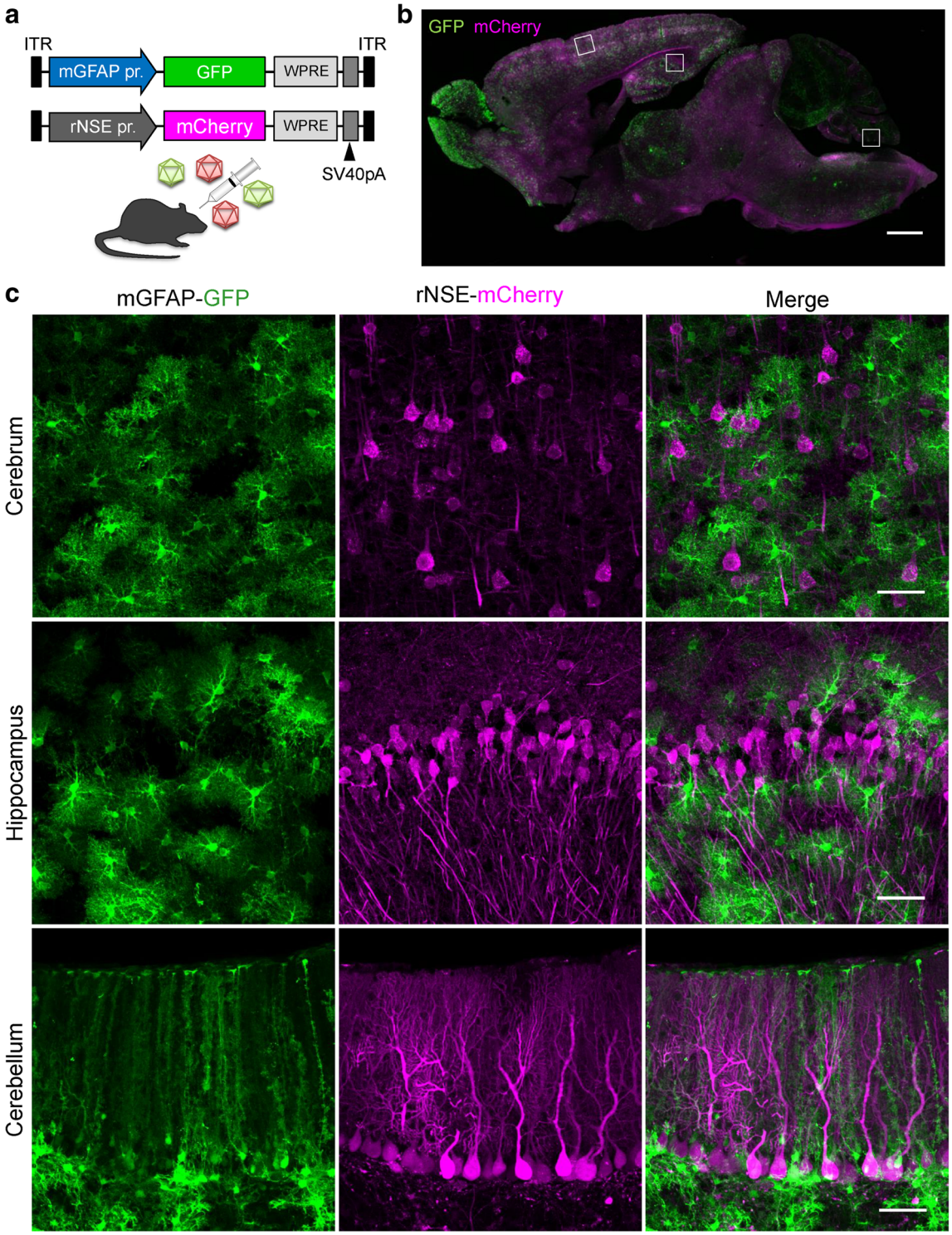

Fig. 2 Distinct transduction of astrocytes and neurons by intravenous injection of a mixture of AAV-PHP.Bs containing astrocyte- or neuron-specific promoters. **a**. Diagram of the AAV vector constructs, which were designed to express either mCherry or GFP under the control of the neuron-specific rNES promoter or the astrocyte-specific mGFAP promoter, respectively. The mixture of the two AAV-PHP.Bs was administered to 5-week-old mice through the orbital sinus, and mice were sacrificed 3 weeks after the injection. **b** A low magnification fluorescent image of the sagittal section immunolabeled for GFP and mCherry. **c** Enlarged immunohistochemical images of GFP and mCherry expression in the boxed regions indicated in **b** (cerebrum, hippocampus, and cerebellum). Scale bars, 1 mm (**b**) and 50 μm (**c**)

of the two fluorescent proteins were examined in different brain regions (boxed areas in Fig. 2b). In the cerebral cortex and the hippocampus, astrocytes and neurons were efficiently and separately labeled by GFP and mCherry, respectively (upper and middle panels in Fig. 2c). In the cerebellar cortex, Bergmann glia and astrocytes expressed GFP, while Purkinje cells expressed mCherry (lower panels in Fig. 2c). These data suggest that AAV-PHP.B can infect various cell types, including neurons and astrocytes, and express GFP or mCherry depending on the cell type.

We recently reported that intravenous injection of AAV-PHP.B failed to show transduction in the marmoset brain [16]. Interestingly, it was reported that systemic injection of AAV-PHP.B failed to cause transduction in the CNS in a commonly used mouse strain, BALB/cJ [18]. Thus, we tested the BBB permeability to AAV-PHP.B in rats. The CD (Sprague Dawley) rats received a systemic injection of AAV-PHP.B or AAV9 vectors (both 3.8–4.7 × 10^{13} vg/kg), at a similar dosage as that used for mice. Three weeks after the injection, brains were examined. Similar to the brains from a non-injected control rat and from a rat treated with AAV9 vectors, the brain from a rat treated with AAV-PHP.B showed little GFP fluorescence, except in the cuneate fasciculus (Supplementary Fig. 1A), which was GFP-labeled presumably by axonal projections from the dorsal root ganglia, as revealed in marmosets [16]. There was statistically no difference in the native GFP fluorescence intensity between AAV-PHP.B-treated brains ($n = 5$) and those treated with AAV9 ($n = 9$) (Supplementary Fig. 1B). Immunohistochemistry for GFP showed GFP-labeled neurons scattered in the cerebral cortex, but the overall density was identical between AAV-PHP.B-treated mice and those treated with AAV9 (Supplementary Fig. 1C). These results suggest that systemically administered AAV-PHP.B only has little potency for CNS transduction in CD (Sprague Dawley) rats, at least with a titer that worked efficiently in C57BL/6 mice.

Time Course of the Production of Neutralizing Antibodies

Intravenous injection of AAV-PHP.B is thought to trigger the production of neutralizing antibodies (NAbs) against the AAV-PHP.B capsid. Accordingly, we examined the increase in NAb titers [immunoglobulin M (IgM) and immunoglobulin G (IgG)] in serum samples collected 1, 2, 3, and 7 days after the AAV-PHP.B injection using an ELISA assay. When the average ELISA absorbance value of the serum samples 7 days after the injection was defined as 100%, the absorbances 1 day after injection were 1.9 ± 0.1% (IgM) and 1.3 ± 0.2% (IgG), which were almost comparable to those from naïve control mice [2.1 ± 0.4% (IgM) and 1.2 ± 0.2% (IgG)]. Two days after the injection, increases in both IgM and IgG became evident [5.8 ± 0.7% (IgM) and 5.3 ± 0.5% (IgG)], and the values increased exponentially thereafter for both antibody types (Fig. 3a, b). A similar time course of increase in IgM and IgG has been observed following infection with different viruses [19].

Pre-treatment of Mice Completely Abolishes the Competence of AAV-PHP.B in 7 Days

Production of NAbs in mice is thought to block subsequent brain transduction by a second intravenous administration of AAV-PHP.B, presumably after some latent period. To examine this, we intravenously injected AAV-PHP.B expressing mCherry under the control of the astrocyte-specific mGFAP promoter, followed by a second intravenous injection with AAV-PHP.B expressing GFP under the control of the neuron-specific NSE promoter, with different time intervals between the two injections (Fig. 4a). The expression levels of GFP 14 days after the second injection were then examined. Mice that received only the second injection of the GFP-expressing virus (i.e., without the first injection of the AAV-PHP.B virus expressing mCherry) showed efficient GFP expression selectively in neurons (Fig. 4b). When the two viruses were simultaneously injected, GFP fluorescence in the brain was almost comparable to that of control mice that received only the second intravenous injection with AAV-PHP.B expressing GFP under the control of the neuron-specific NSE promoter (Fig. 4c). Intravenous injection of the two different viruses with a 1-day interval caused a moderate decrease in brain transduction after the second injection (Fig. 4d). Attenuation of brain transduction following the second injection became noticeable after a 2-day interval, and GFP expression following the second viral injection became almost and completely undetectable at intervals of 3 days and 7 days (Fig. 4e–g). These qualitative conclusions were substantiated by a quantitative analysis of GFP fluorescence intensity in AAV-PHP.B-treated whole brains ($n = 4$ mice, Fig. 5). A comparison of GFP fluorescence in the brain with the serum NAb levels (Figs. 3 and 5) indicates that the undetectable levels of NAbs begin to suppress brain transduction by AAV-PHP.B from as early as 1 day after intravenous administration, and the barely detectable levels of NAbs at 2 days post-viral injection significantly abolish the capability of intravenously administered AAV-PHP.B for CNS transduction. The capacity of a second injection of AAV-PHP.B to transduce the brain with a transgene was almost and fully eliminated after 3- or 7-day intervals.

Treatment with Cyclosporine Fails to Circumvent the Production of NAbs

We examined whether pharmacological immunosuppression enabled second AAV-PHP.B-mediated transgene expression with a 1-week interval between injections. Mice were

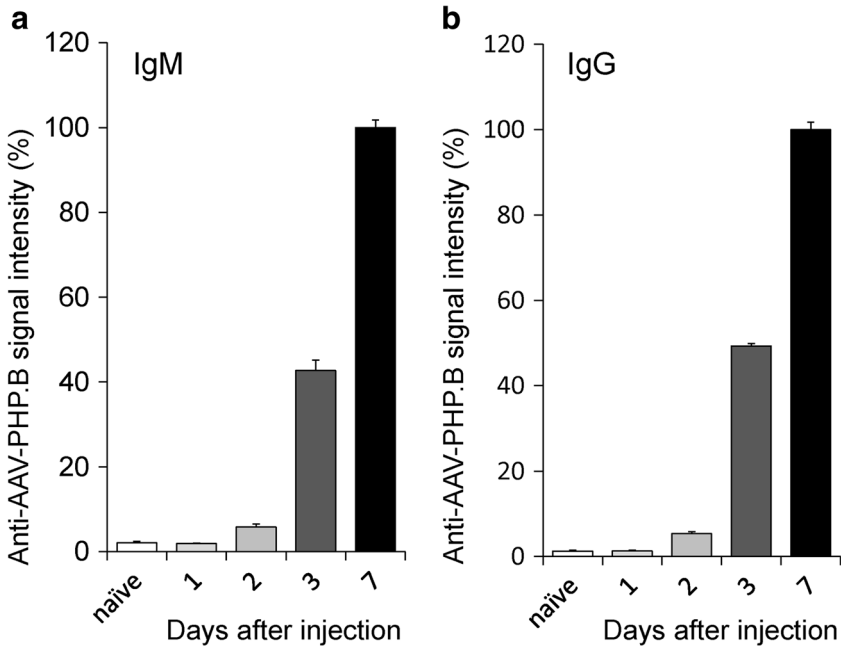

Fig. 3 Time course of the onset of AAV-PHP.B neutralizing activity in the serum of mice that had received AAV-PHP.B. Sera were obtained from mice 1, 2, 3, or 7 days post-intravenous injection of AAV-PHP.B; sera from naïve mice was used as the control. The levels of neutralizing antibodies against the AAV-PHP.B capsid were assessed by ELISA. **a** Time course of IgM production. **b** Time course of IgG production. The assay was performed in duplicate for each mouse, using three mice for each point. The average absorbance value of samples collected 7 days after AAV-PHP.B injection was defined as 100%. ELISA enzyme-linked immunosorbent assay

intraperitoneally treated with cyclosporine (20 g/kg) once a day for 1 week, and received a systemic injection of AAV-PHP.B expressing mCherry (Supplemental Fig. 2A). Treatment with cyclosporine was continued for one more week (for a total of 2 weeks), and then the mice received a second systemic injection of AAV-PHP.B expressing GFP. Two weeks after the second injection, we found mCherry expression owing to the first injection throughout the brain, but no GFP expression owing to the second injection (Supplemental Fig. 2B–F), suggesting that cyclosporine did not effectively suppress the production of the NAbs.

Direct Cortical Injection of AAV-PHP.B Can Transduce the Brain in Seropositive Mice

The above data indicate that pre-existing NAbs against AAV-PHP.B strongly inhibit transgene expression by intravenously administered AAV-PHP.B, which poses a significant hurdle to using AAV vectors in seropositive animals. To examine whether a direct injection into the brain parenchyma allows for successful expression of a transgene in seropositive animals, we injected AAV-PHP.B expressing GFP directly into the cerebellar cortex of mice that had been systemically treated with AAV-PHP.B 1 week prior to the second injection. The mice were sacrificed 2 weeks after the second injection (Fig. 6A (a)). As a result, we observed bright GFP fluorescence in the cerebellum (Fig. 6A (b)). The sagittal section also showed efficient expression of mCherry and GFP (Fig. 6A (c, d)), indicating the effectiveness of brain parenchymal injection for transgene expression in mice seropositive for the AAV-PHP.B capsid. In contrast, direct cerebellar cortical injection followed by systemic injection of AAV-PHP.B, with a 1-week interval between injections, resulted in a suppression of the expression of the second transgene (Fig. 6B). Essentially identical results were obtained by direct injection into the cerebral cortex or by intracerebroventricular injection, followed by systemic injection (Supplementary Fig. 3). These results suggest that AAV-PHP.B released into the CSF enters peripheral circulation and produces NAbs. To validate this, we injected AAV-PHP.B intravenously or directly into the cerebellar cortex and measured the NAbs in both the serum and CSF of the mice 1 week after the injection. Intravenous injection of AAV-PHP.B consistently produced NAbs in the serum, but had no influence on NAb level in the CSF (Fig. 6C). As expected, direct cortical injection of AAV-PHP.B increased NAb production in the serum without affecting NAb level of CSF (Fig. 6D). Collectively, our results indicate that serum NAbs against AAV-PHP.B, which are produced upon viral exposure to the peripheral circulation or CSF, cannot enter the brain, and thus, transgene expression by AAV vectors can be attained by direct injection of AAV vectors into the brain tissue or ventricle even in the presence of NAbs in the serum.

Discussion

AAV-PHP.B can permeate the mouse BBB, and attain a broad transduction of the CNS [11]. Here, we demonstrated that AAV-PHP.Bs carrying the rNSE or mGFAP promoters resulted in the specific transduction of neurons or astrocytes, respectively. The cell type specific expression was not disrupted by mixing two AAV-PHP.Bs carrying different promoters: neurons were specifically transduced

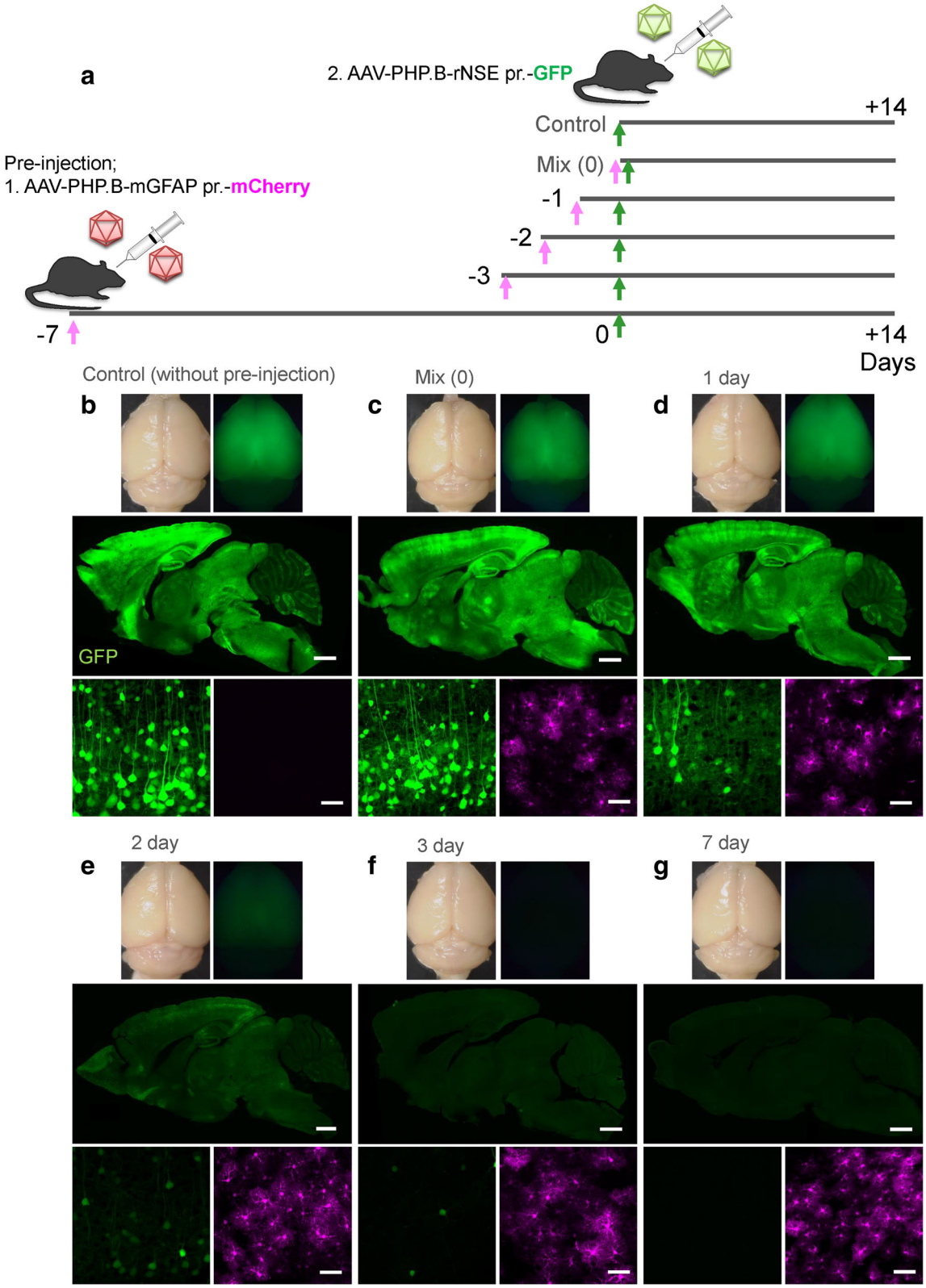

by AAV-PHP.Bs expressing mCherry under the control of the rNSE promoter, and astrocytes were specifically transduced with AAV-PHP.Bs expressing GFP under the control of mGFAP promoter, with no cross-expression of the two transgenes noted. Thus, AAV-PHP.Bs carrying cell type-specific promoters are useful for the global transduction of specific cell populations in the CNS and so could

◀ **Fig. 4** Immune-mediated suppression of CNS transduction by intravenously administered AAV-PHP.B. **a** Schematic of the schedule for intravenous injection of the two different AAV-PHP.Bs (first injection, AAV-PHP.B-mGFAP pr.-mCherry, second injection AAV-PHP.B-rNSE pr.-GFP, 1.0×10^{12} vg) with different intervals between the two injections. Five-week-old wild-type mice received an intravenous injection of AAV-PHP.B expressing mCherry under the control of the mGFAP promoter or AAV-PHP.B expressing GFP under the control of the rNSE promoter either simultaneously, or with intervals of 1, 2, 3, or 7 days between the first injection and the second injection, as indicated. The mice were sacrificed 14 days after the second injection. Control mice received only the second injection. **b**–**g** Decrease and eventual loss of GFP expression as the interval between injections becomes longer. The upper panel sets are bright field (left) and GFP fluorescence (right) images of the whole brains, and the middle panels are the native GFP fluorescence images of the sagittal sections. The lower panel sets show the enlarged GFP (left) and mCherry (right) images of the cerebral cortex. The intervals between the two intravenous injections are displayed above the respective whole brain images. Scale bars, 1 mm (**b**–**g**, middle) and 50 μm (**b**–**g**, lower)

contribute significantly in advancing neuroscience research.

One major hurdle to overcome is the production of NAbs that eliminate intravenously administered AAV-PHP.B. The brains of mice in our breeding colony were universally and almost identically transduced by intravenously

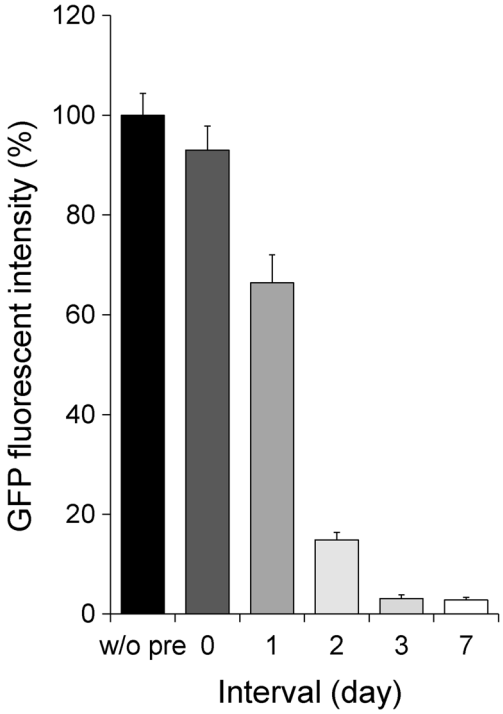

Fig. 5 Summary graph showing the exponential decrease in expression of the second transgene (GFP) as the length of time between the two AAV-PHP.B injections increased. The GFP fluorescence intensity of the whole brain was measured using ImageJ software. At each experimental time point, four mice were measured, and the average intensity was normalized with that obtained from the control mice that received only a single injection of AAV-PHP.B expressing GFP under the control of the rNSE promoter. w/o pre without pre-injection

administered AAV-PHP.B, indicating that naïve mice in our breeding colony were seronegative for AAV-PHP.B and also probably for the natural AAV9 capsid (AAV-PHP.B has only a seven amino acid insertion in the AAV9 capsid). Under these circumstances, intravenous injection of AAV-PHP.B into mice triggered an exponential increase in NAb levels, which became detectable by ELISA 2 days after viral injection, and rapidly increased thereafter (Fig. 3). Indeed, intravenous administration of AAV-PHP.B expressing GFP 2 days after pre-treatment with AAV-PHP.B resulted in ~80% reduction of GFP expression (Fig. 5). Although a significant increase in NAbs was not detected on the day following intravenous administration, a second injection of AAV-PHP.B was able to cause a significant reduction in GFP expression of 65% of the control level (Figs. 3 and 5). These data suggest that preclusion of AAV-PHP.B starts as early as the first day after immunization, is nearly complete by 3 days, and becomes perfect after 1 week.

Our data showed that AAV-PHP.B carrying cell type-specific promoters can deliver genes via peripheral veins to the CNS and express them in specific cell populations. Transgenes that could potentially be expressed by AAV-PHP.B include mutant genes responsible for brain disorders, miRNAs (knock-down), and gene sets that can edit the host genome (knock-out or knock-in). AAV vector-mediated transgene expression was demonstrated in one study to continue even at 1 year post-injection in mice [20] and at 15 years in the postmortem brain of a cynomolgus macaque [21]. Thus, global, efficient, and persistent gene modification mediated by AAV-PHP.B in a brain cell type-specific manner should allow us to generate animal models of various types of brain disorders, which should be useful for therapeutic intervention studies. However, the generation of NAbs in peripheral circulation impedes the repeated use of AAV-PHP.B for further transduction of the brain. One idea to circumvent the production of NAbs is to inject the AAV vectors directly into the brain parenchyma. To validate this idea, we injected AAV-PHP.B expressing GFP into the cerebellar parenchyma 1 week after the systemic injection of AAV-PHP.B expressing mCherry. Parenchymal injection of AAV-PHP.B led to an efficient expression of GFP, even in the presence of the NAbs in the peripheral blood circulation. ELISA assay revealed that serum NAbs could not enter the brain (Fig. 6C). In contrast, using a reverse injection order, i.e., brain parenchymal injection followed by systemic injection after a 1-week interval, selectively eliminated the second transduction in the brain. We showed that AAV-PHP.B injection into the brain tissue caused NAb production in the serum (Fig. 6D). These results suggest that AAV-PHP.B particles injected into the brain parenchyma or lateral ventricle enter peripheral circulation likely

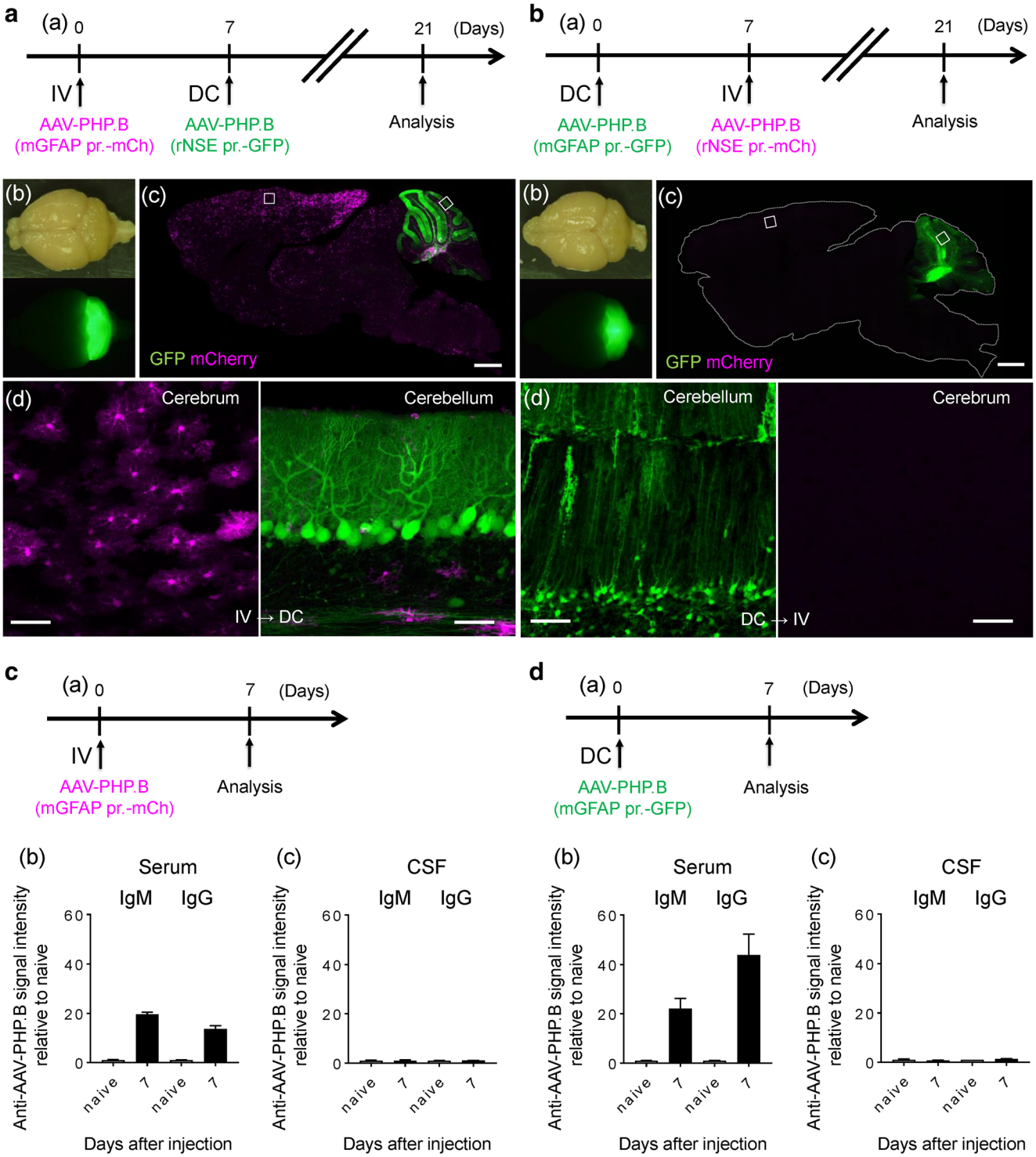

through the glymphatic system [22, 23], leading to the production of NAbs, resulting in the neutralization of subsequently injected AAV-PHP.B.

Our recent study indicated that, unlike in mice, AAV-PHP.B shows little superiority over AAV9 vectors in non-human primates (NHPs) in terms of CNS transduction following systemic administration [12, 16]. This was also demonstrated in rats (Supplementary Fig. 1). In analogy with NHPs, AAV-PHP.B presumably shows little permeability of the human BBB. Thus, development of AAV variants with a high penetrance of the human BBB will be required for intravenous

◀ **Fig. 6** Direct cortical injection circumvents NAbs. (A-a) Schema depicting the experimental design. AAV-PHP.B expressing GFP under the control of the rNSE promoter was directly injected into the cerebellar parenchyma (direct cortical injection; DC) 7 days after the intravenous administration of AAV-PHP.B expressing mCherry under the control of the mGFAP promoter (intravenous injection; IV). GFP and mCherry expression in the brain were examined 2 weeks after the second injection. (A-b) Bright field (upper) and fluorescent (lower) images of the whole brain, showing robust GFP expression in the cerebellum. (A-c) The sagittal section double immunolabeled for GFP and mCherry. (A-d) Magnified images of the cerebrum (left) and cerebellum (right) corresponding to the boxed regions depicted in (A-c). (B-a) Reversal of the injection order: AAV-PHP.B expressing GFP under the control of the mGFAP promoter was directly injected into the cerebellar parenchyma (DC). Seven days after the direct cortical injection, AAV-PHP.B expressing mCherry under the control of the rNSE promoter was injected intravenously (IV). (B-b) Bright field (upper) and fluorescent (lower) images of the whole brain, showing robust GFP expression in the cerebellum. (B-c) The sagittal section double immunolabeled for GFP and mCherry. (B-d) Magnified images of the cerebellum (left) and cerebrum (right) corresponding to the boxed regions depicted in (B-c). Note the absence of mCherry expression after the second intravenous AAV-PHP.B injection in a mouse that had received cerebellar parenchymal injection of AAV-PHP.B. Scale bars, 1 mm (A-c and B-c) and 50 μm (A-d and B-d). (C, D) Experimental schema (a) and levels of NAbs in the serum (b) and CSF (c). Mice received intravenous injection (C) or direct cerebellar injection (D) of AAV-PHP.B, and NAb levels (IgM and IgG) in both the serum and CSF were measured 1 week after the injection

administration-based gene therapy targeting human brain diseases. In addition, approximately 80% of the human population is seropositive for any of the AAV serotypes [2], indicating that an assessment of pre-existing antibodies will be a prerequisite before systemic application of AAV vectors. Even in immunologically naïve people, a single systemic application of an AAV vector will generate NAbs, precluding repeated viral administration. Therefore, in parallel with development of AAV variants permeable to the human BBB, approaches to circumvent NAbs should be established in order to expand the number of patients. Although this is not a fundamental resolution, our present results indicate a possible approach to that end, through the direct application of AAV vectors into the brain tissue or ventricle, because serum NAbs do not impede directly injected AAV vectors from inducing transduction in the brain.

Acknowledgments We thank Asako Ohnishi and Junko Sugiyama for the viral vector production and the maintenance of mice.

Author Contributions YS designed and performed the experiments, analyzed the data, and drafted the manuscript. AK designed the experiments and contributed to production of AAV vectors. KN (ELISA), YM (experiments using rats), and HY (immunohistochemistry) performed the experiments. JS and KH supervised the ELISA experiment. HH designed the experiments and wrote the manuscript.

Funding Information This research was supported by the program for Brain Mapping by Integrated Neurotechnologies for Disease Studies (Brain/MINDS) from Japan Agency for Medical Research and Development, AMED, under the Grant Number JP17dm0207057h0001 (to H. Hirai), and partially supported by JSPS KAKENHI Grant Number 15K18330 (to A. Konno) and 17K14929 (to Y. Matsuzaki).

Compliance with Ethical Standards

Competing Interests The authors declare that they have no competing interests.

References

1. Atchison RW, Casto BC, Hammon WM (1965) Adenovirus-associated defective virus particles. Science (New York, NY) 149(3685):754–756
2. Weitzman MD, Linden RM (2011) Adeno-associated virus biology. Methods Mol Biol (Clifton, NJ) 807:1–23. https://doi.org/10.1007/978-1-61779-370-7_1
3. Saraiva J, Nobre RJ, Pereira de Almeida L (2016) Gene therapy for the CNS using AAVs: the impact of systemic delivery by AAV9. J Control Release 241:94–109. https://doi.org/10.1016/j.jconrel.2016.09.011
4. Srivastava A (2016) In vivo tissue-tropism of adeno-associated viral vectors. Curr Opin Virol 21:75–80. https://doi.org/10.1016/j.coviro.2016.08.003
5. Arsenault J, Gholizadeh S, Niibori Y, Pacey LK, Halder SK, Koxhioni E, Konno A, Hirai H et al (2016) FMRP expression levels in mouse central nervous system neurons determine behavioral phenotype. Hum Gene Ther 27(12):982–996. https://doi.org/10.1089/hum.2016.090
6. Huda F, Konno A, Matsuzaki Y, Goenawan H, Miyake K, Shimada T, Hirai H (2014) Distinct transduction profiles in the CNS via three injection routes of AAV9 and the application to generation of a neurodegenerative mouse model. Mol Ther Methods Clin Dev Article number: 14032. https://doi.org/10.1038/mtm.2014.32
7. Matsuzaki Y, Konno A, Mukai R, Honda F, Hirato M, Yoshimoto Y, Hirai H (2016) Transduction profile of the marmoset central nervous system using adeno-associated virus serotype 9 vectors. Mol Neurobiol 54:1745–1758. https://doi.org/10.1007/s12035-016-9777-6
8. Bevan AK, Duque S, Foust KD, Morales PR, Braun L, Schmelzer L, Chan CM, McCrate M et al (2011) Systemic gene delivery in large species for targeting spinal cord, brain, and peripheral tissues for pediatric disorders. Mol Ther 19(11):1971–1980. https://doi.org/10.1038/mt.2011.157
9. Gray SJ, Matagne V, Bachaboina L, Yadav S, Ojeda SR, Samulski RJ (2011) Preclinical differences of intravascular AAV9 delivery to neurons and glia: a comparative study of adult mice and nonhuman primates. Mol Ther 19(6):1058–1069. https://doi.org/10.1038/mt.2011.72
10. Samaranch L, Salegio EA, San Sebastian W, Kells AP, Foust KD, Bringas JR, Lamarre C, Forsayeth J et al (2012) Adeno-associated virus serotype 9 transduction in the central nervous system of nonhuman primates. Hum Gene Ther 23(4):382–389. https://doi.org/10.1089/hum.2011.200
11. Deverman BE, Pravdo PL, Simpson BP, Kumar SR, Chan KY, Banerjee A, Wu WL, Yang B et al (2016) Cre-dependent selection yields AAV variants for widespread gene transfer to the adult brain. Nat Biotechnol 34(2):204–209. https://doi.org/10.1038/nbt.3440
12. Nitta K, Matsuzaki Y, Konno A, Hirai H (2017) Minimal Purkinje cell-specific PCP2/L7 promoter virally available for rodents and non-human primates. Mol Ther Methods Clin Dev 6:159–170. https://doi.org/10.1016/j.omtm.2017.07.006

13. Shinohara Y, Konno A, Takahashi N, Matsuzaki Y, Kishi S, Hirai H (2016) Viral vector-based dissection of marmoset GFAP promoter in mouse and marmoset brains. PLoS One 11(8):e0162023. https://doi.org/10.1371/journal.pone.0162023
14. Yeo S, Bandyopadhyay S, Messing A, Brenner M (2013) Transgenic analysis of GFAP promoter elements. Glia 61(9): 1488–1499. https://doi.org/10.1002/glia.22536
15. Shinohara Y, Ohtani T, Konno A, Hirai H (2017) Viral vector-based evaluation of regulatory regions in the neuron-specific enolase (NSE) promoter in mouse cerebellum in vivo. Cerebellum (London, England). https://doi.org/10.1007/s12311-017-0866-5
16. Matsuzaki Y, Konno A, Mochizuki R, Shinohara Y, Nitta K, Okada Y, Hirai H (2018) Intravenous administration of the adeno-associated virus-PHP.B capsid fails to upregulate transduction efficiency in the marmoset brain. Neurosci Lett 665:182–188. https://doi.org/10.1016/j.neulet.2017.11.049
17. Samaranch L, Blits B, San Sebastian W, Hadaczek P, Bringas J, Sudhakar V, Macayan M, Pivirotto PJ et al (2017) MR-guided parenchymal delivery of adeno-associated viral vector serotype 5 in non-human primate brain. Gene Ther 24(4):253–261. https://doi.org/10.1038/gt.2017.14
18. Hordeaux J, Wang Q, Katz N, Buza EL, Bell P, Wilson JM (2018) The neurotropic properties of AAV-PHP.B are limited to C57BL/6J mice. Mol Ther 26(3):664–668. https://doi.org/10.1016/j.ymthe.2018.01.018
19. Guzman MG, Halstead SB, Artsob H, Buchy P, Farrar J, Gubler DJ, Hunsperger E, Kroeger A et al (2010) Dengue: a continuing global threat. Nat Rev Microbiol 8(12 Suppl):S7–S16. https://doi.org/10.1038/nrmicro2460
20. Jiang L, Zhang H, Dizhoor AM, Boye SE, Hauswirth WW, Frederick JM, Baehr W (2011) Long-term RNA interference gene therapy in a dominant retinitis pigmentosa mouse model. Proc Natl Acad Sci U S A 108(45):18476–18481. https://doi.org/10.1073/pnas.1112758108
21. Sehara Y, Fujimoto KI, Ikeguchi K, Katakai Y, Ono F, Takino N, Ito M, Ozawa K et al (2017) Persistent expression of dopamine-synthesizing enzymes 15 years after gene transfer in a primate model of Parkinson's disease. Human gene therapy Clinical development 28(2):74–79. https://doi.org/10.1089/humc.2017.010
22. Bacyinski A, Xu M, Wang W, Hu J (2017) The Paravascular pathway for brain waste clearance: current understanding, significance and controversy. Front Neuroanat 11:101. https://doi.org/10.3389/fnana.2017.00101
23. Louveau A, Plog BA, Antila S, Alitalo K, Nedergaard M, Kipnis J (2017) Understanding the functions and relationships of the glymphatic system and meningeal lymphatics. J Clin Invest 127(9):3210–3219. https://doi.org/10.1172/jci90603